Supporting information

A highly-active $Zn_{0.58}Co_{2.42}O_4$ spinel oxide as a promising cathode for proton-conducting solid oxide fuel cells

Yangsen Xu [a], Yueyuan Gu [a, *] and Lei Bi [a, *]

a. School of Resource Environment and Safety Engineering, University of South China, Hengyang 421001, China

*Corresponding author

Email: guyueyuan@usc.edu.cn (Y.Y. Gu)

lei.bi@usc.edu.cn, bilei81@gmail.com (L. Bi)

Experimental section

ZCO spinel oxide and perovskite-based LSCF were synthesized by a conventional combustion method,[1] which used $Zn(NO_3)_2$, $Co(NO_3)_3$, La_2O_3, $SrCO_3$, and $Fe(NO_3)_3$ as the starting materials. ZCO and LSCF materials were fired at 950 ℃ for 3 h. The powder phase structure was examined by X-ray diffraction (XRD, DX-2700BH, Haoyuan Instrument). The chemical stability of ZCO spinel powder was evaluated through in-situ high-temperature XRD, which involved the treatment of ZCO material at a high temperature (600℃) with a flowing rate of 30 mL min^{-1}10%CO_2-90%air mixture gas. At the same time, the XRD data of the sample were recorded. The chemical phase structure stability of the ZCO powder from 100 to 900℃ was also measured by in-situ high-temperature XRD. The morphology and the elements distribution of the ZCO powder were observed through scanning transmission electron microscopy. (STEM, JEM-2100F). In addition, the chemical states of ZCO and LSCF can be analyzed by X-ray photoelectron spectroscopy (XPS, Thermo Fisher ESCALAB 250Xi).

The density functional theory (DFT) method based on the first-principles calculation was carried out to discuss the properties of the ZCO spinel oxides on the atomic level using the VASP software (Vienna ab initio simulation package).[2-5] The cutoff energy was set to 520 eV, and a gamma centered 4×4×4 K-point mesh was used. The convergence criteria for energy and force were 10^{-5} eV and 0.05 eV °A^{-1}, respectively. The U correction value of 3.32 eV and 4 eV was added to Co and Fe, respectively. The 2 × 1 × 1 and 2 × 2 × 2 supercells were used for the calculation of

ZCO and LSCF, respectively. For the calculation of the surface of ZCO and LSCF, the vacuum layer with a thickness of 15 Å was constructed. The calculation details of oxygen vacancy formation energy and hydration energy can be found in previous studies.[6, 7]

In the electrochemical performance tests, ZCO and LSCF cathode ink was brushed on the dense BCZY electrolyte membrane separately, then calcined in the microwave furnace at 900℃ for 10 minutes. The half-cell was constituted of a dense BZCY electrolyte membrane and the NiO-BCZY anode followed the co-pressing and co-sintering method. BCZY electrolyte powder was obtained by the modified sol-gel method. NiO-BCZY was prepared by mixing the pure phase BCZY powder with the NiO powder in a weight ratio of 4 to 6. The half-cells were sintered at 1300 ℃ for 6 h in the furnace to acquire the dense electrolyte, and the detailed fabrication methods also can be found in our previous works.[8] The electrochemical performance of the ZCO and LSCF cathode was tested at different temperatures (700, 650, and 600 ℃) using wet H_2 (3% H_2O) as the fuel gas while the static air at the cathode side. The performance of cells was measured through an electrochemical workstation (Squidstat Plus, Admiral Instrument), and the electrochemical impedance spectroscopy (EIS) was tested under the open circuit voltage from 1 M Hz to 0.1 Hz. The electrical conductivity relaxation (ECR) method was applied in evaluating the oxygen (or proton) surface exchange coefficient and diffusion coefficient of ZCO and LSCF. The four-probe method was exploited to monitor the conductivity and time for ZCO and LSCF bars in reaching equilibrium when the gas was abruptly switched.

References

1. X. Xu, L. Bi and X. S. Zhao, *J Membrane Sci*, 2018, **558**, 17-25.

2. G. Kresse and D. Joubert, *Phys Rev B*, 1999, **59**, 1758-1775.

3. G. Kresse and J. Furthmuller, *Phys Rev B*, 1996, **54**, 11169-11186.

4. P. E. Blöchl, O. Jepsen and O. K. Andersen, *Phys Rev B*, 1994, **49**, 16223-16233.

5. W. Kohn and L. J. Sham, *Phys Rev*, 1965, **140**, A1133-A1138.

6. X. Xu, H. Q. Wang, J. M. Ma, W. Y. Liu, X. F. Wang, M. Fronzi and L. Bi, *J Mater Chem A*, 2019, **7**, 18792-18798.

7. X. K. Lu, X. Yang, L. C. Jia, B. Chi, J. Pu and J. Li, *Int. J. Hydrogen Energy*, 2019, **44**, 16359-16367.

8. B. Wang, X. H. Liu, L. Bi and X. S. Zhao, *J. Power Sources*, 2019, **412**, 664-669.

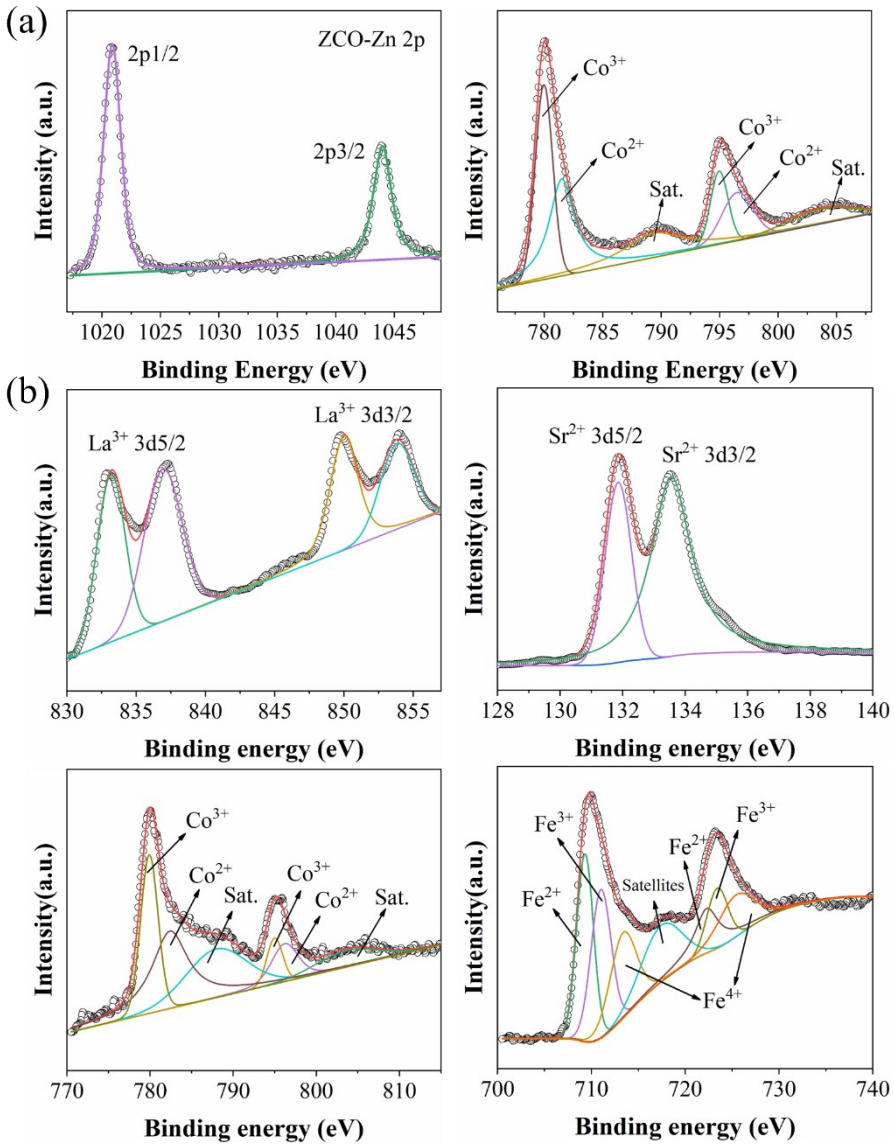

Figure S1. XPS spectra for the elements in (a) ZCO and (b) LSCF.

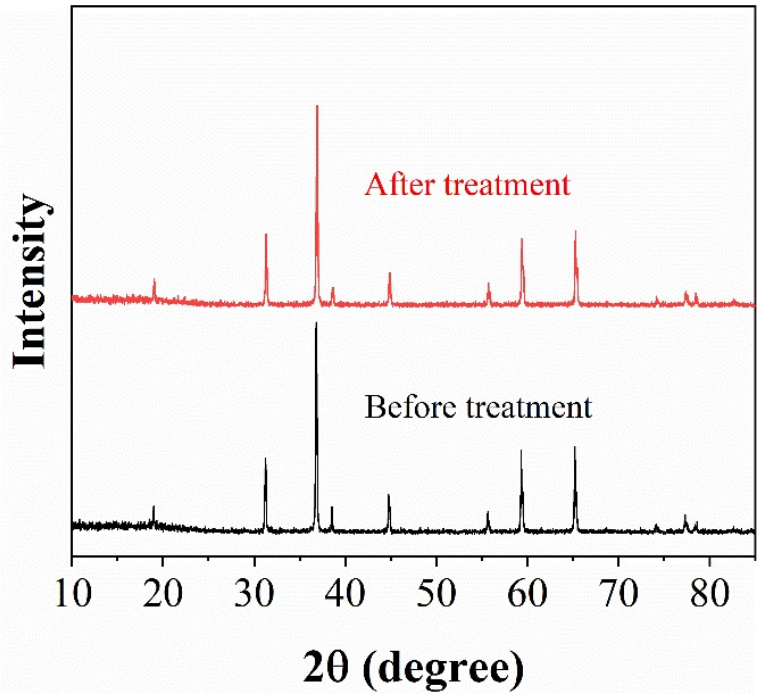

Figure S2. XRD patterns for ZCO powder before and after the treatment in a 30% H_2O-containing atmosphere at 600 °C for 10 h.

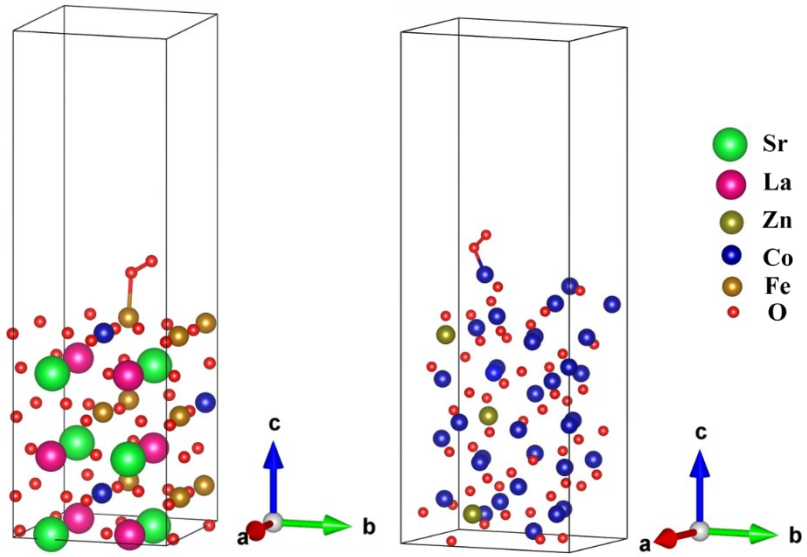

Figure S3. DFT calculated configurations for O_2 adsorbed LSCF and ZCO.

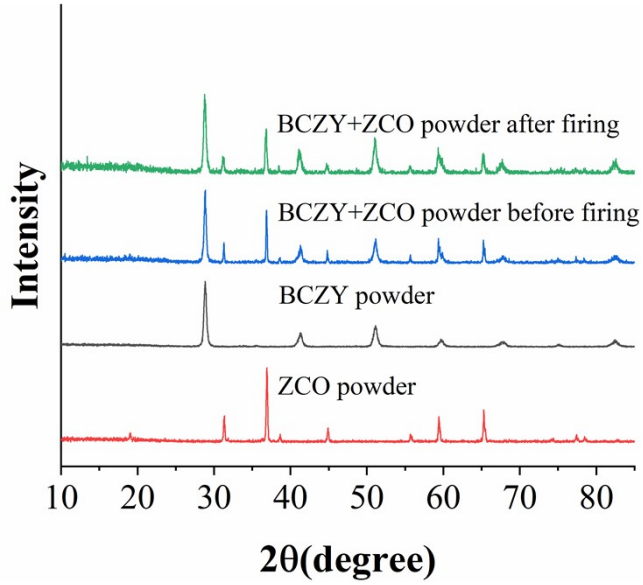

Figure S4. XRD patterns for the as-prepared ZCO and BCZY powders, and the BCZY+ZCO composite powder before and after firing.

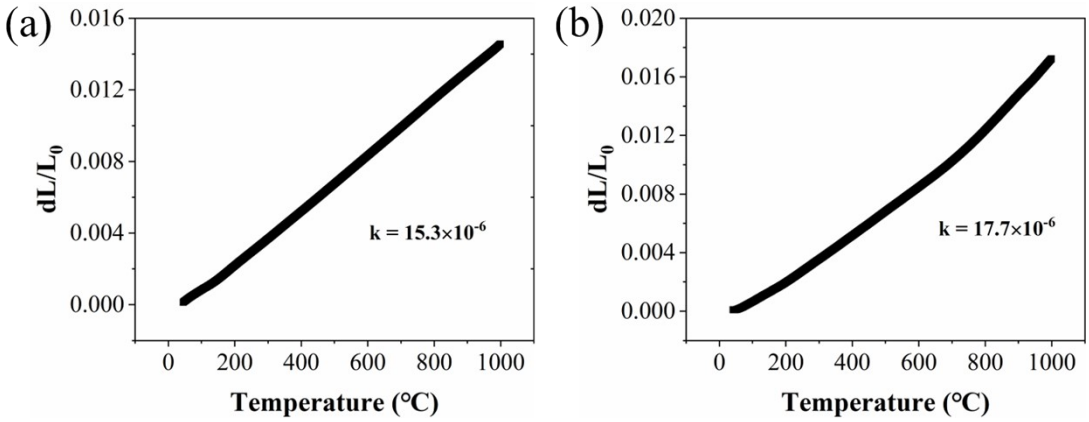

Figure S5. Thermal expansion coefficient (TEC) for (a) ZCO and (b) LSCF was tested from room temperature to 1000 °C.

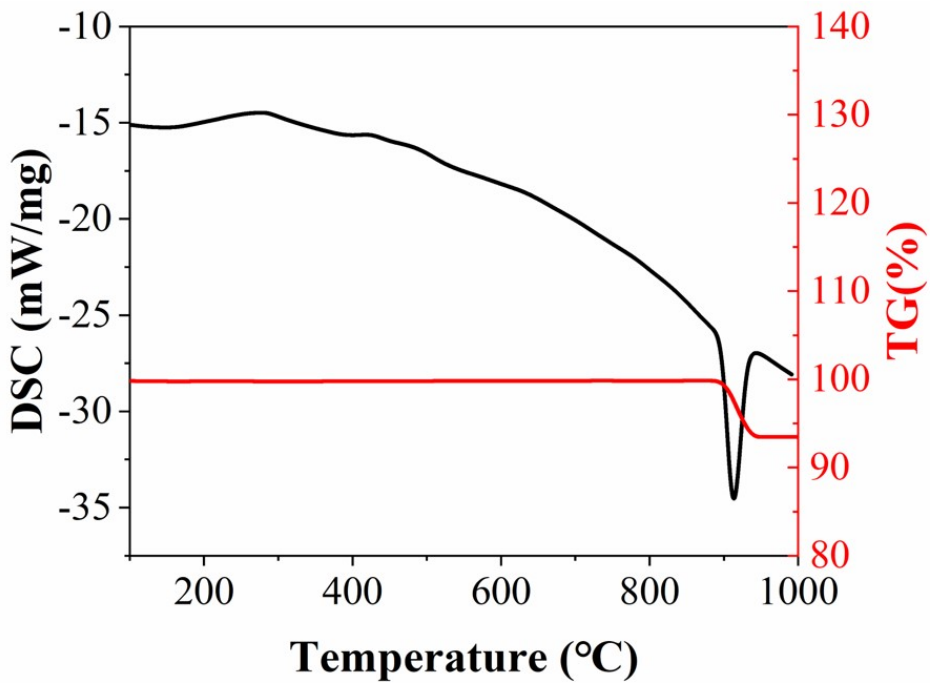

Figure S6. TG-DSC curves of ZCO powder in flowing dry air.

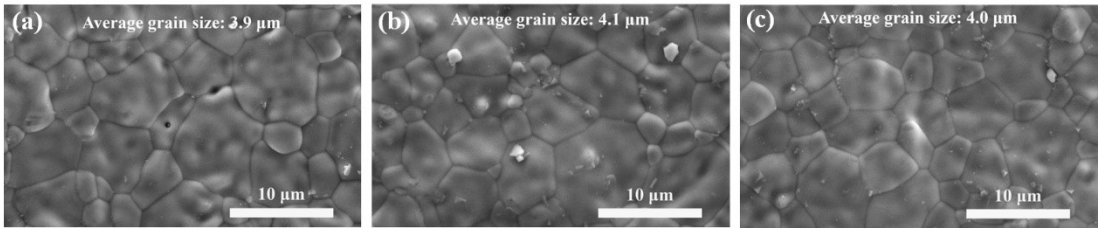

Figure S7. The electrolyte surface of the (a) ZCO-800, (b) ZCO-900, and (c) ZCO-1000.

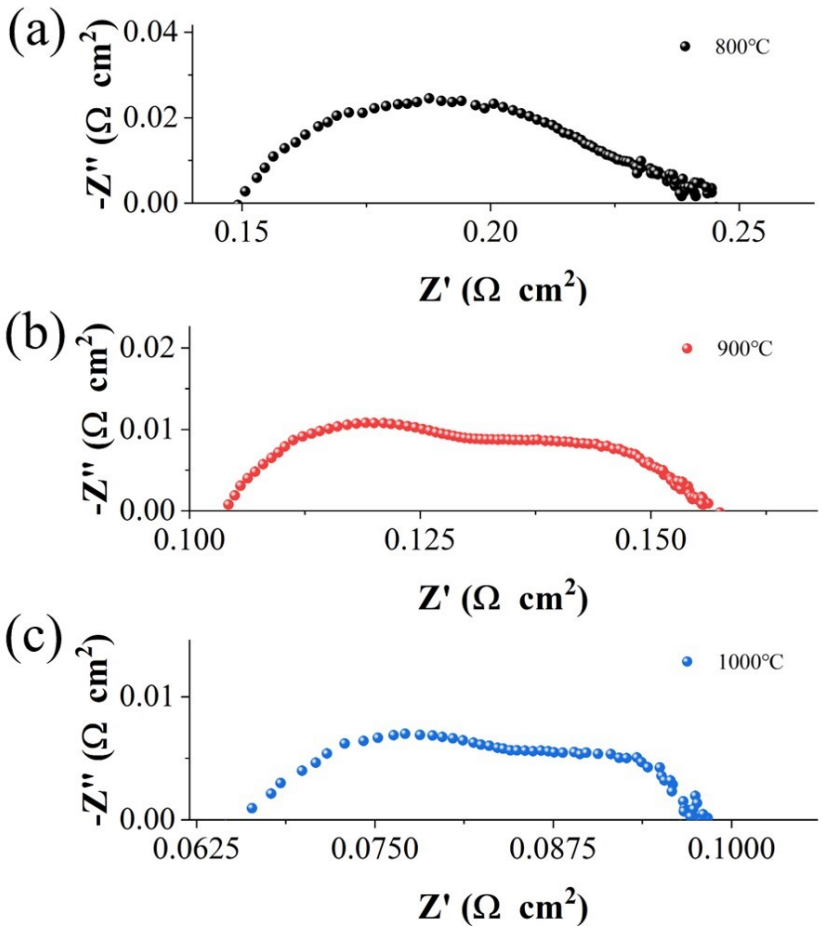

Figure S8. EIS plots for the ZCO cell co-fired at (a) 800, (b) 900 and (c) 1000 °C. The testing temperature is 700 °C.

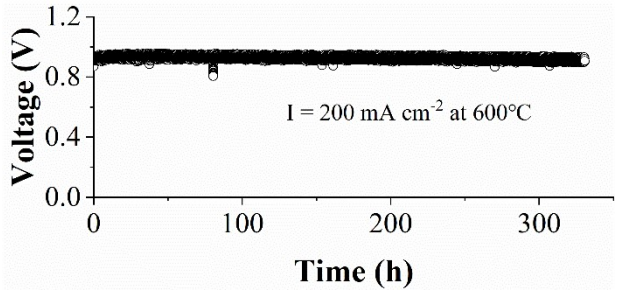

Figure S9. Long-time stability of ZCO cell tested at 600℃ under a constant density of 200 mA cm^{-2}.

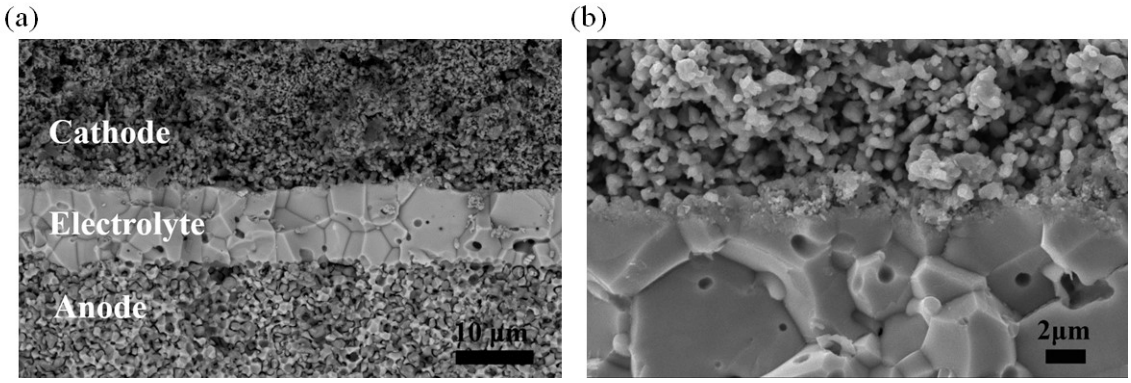

Figure S10. SEM images for the cell after the long-term stability test: (a) the complete cell, (b) the cathode/electrolyte interface.